Study On Cobalt Free Hardfacing Materials For Wear Resistance In Sodium Fast Reactors

P. Aubry, M. Blanc, F. Rouillard, G. Rolland, T. Marlaud, R. Robin, H. Maskrot, M. Blat-Yriex, L. Nicolas

Proceedings of ICAPP 2017

April 24-28, 2017 - Fukui and Kyoto (Japan)

STUDY ON COBALT FREE HARDFACING MATERIALS FOR WEAR RESISTANCE IN SODIUM FAST REACTORS

Pascal Aubry[1], Cécile Blanc[1], Fabien Rouillard[2], Gilles Rolland[3], Thorsten Marlaud[4], Raphael Robin[2], Hicham Maskrot[1], Martine Blat-Yrieix[3], Laetitia Nicolas[5]

1 Den – Service d'Etudes Analytiques et de Réactivité des Surfaces (SEARS), CEA, Université Paris-Saclay, F-91191, Gif sur Yvette, France, pascal.aubry@cea.fr

2 Den – Service de la Corrosion et du Comportement des Matériaux dans leur Environnement (SCCME), CEA, Université Paris-Saclay, F-91191, Gif sur Yvette, France,

3 EDF R&D, Département MMC. Site des Renardières, Ecuelles 77818, Moret-sur-Loing, France

4 AREVA NP, 10 Rue Juliette Récamier, 69006 Lyon, France

5 Den – Département des Matériaux pour le Nucléaire, CEA, Université Paris-Saclay, F-91191, Gif sur Yvette, France,

In this article, we present the ongoing study concerning the selection of cobalt free hardfacing materials for wear resistance in the French Sodium Fast Neutron Reactor ASTRID, currently under development. In the reactor, some parts can be submitted to sliding contact between each other. On these parts, the contact areas usually need a hardfacing coating. The standard hardfacing alloy is a cobalt-base alloy (as, for example Stellite®6). Unfortunately, in the primary coolant circuit and on wear conditions, cobalt can be released. Under neutron flux, the ^{59}Co, stable, can be transmuted into ^{60}Co by neutrons irradiation and, therefore, can contaminate the primary circuit and will be an issue for deconstruction. Therefore, it is desired to replace this cobalt based hardfacing alloy by a cobalt-free one. First, we present the selection of some promising materials and processes selected from the bibliography and previous achieved works. Two processes are used for manufacturing the clads: Plasma Transferred Arc and the Laser Cladding. From the bibliography, different nickel base alloys have been selected. In the presentation, we consider our investigations made on Colmonoy 5. The cobalt base alloy Stellite 6 is evaluated as the reference. The microstructure of the Colmonoy 5 is compared for the two processes. Then, different properties of the clad are evaluated by mechanical, aging, and wear tests. In the project, two tribometers based on planar and linear sliding at high temperature have been set up: one under inert gas protection and one under liquid sodium at operating temperature. After the presentation of the tribometers, wear tests are presented and the wear behavior of the Colmonoy 5 deposits is discussed. Finally, conclusion is given on the quality of the material to be a substitute of cobalt base material.

I. INTRODUCTION

The main feature of Fast Neutron Reactors in the field of tribology is due to the use of an alkali metal as a coolant such as liquid sodium for Sodium Fats Reactors (SFR). The liquid sodium has the ability to reduce many metal oxides. This avidity depends on the nature of the oxides, and the temperature. For reasons related on one hand to the risk of clogging of pipes and on the other hand to corrosion and transfer of activation products, it is necessary to purify the primary and secondary sodium by passing it through cold traps. Thus, a lower temperature is maintained during operation for sealing as the impurity concentration (oxygen and hydrogen) is in the sodium lower itself.

This purification increases the capacity of oxidation-reduction of sodium in particular against the oxides present on the surface of materials and whose influence on the friction is generally favorable. Similarly, the more the purification is pushed towards the low concentrations of oxygen, the less the formation of self-lubricant mixed oxides such as chromite or sodium aluminate is probable. Therefore, the minimum concentration of oxygen in the sodium is fundamental for tribology.

Among the first hard coatings used to overcome the problems of friction in sodium include cobalt based alloys, commonly used in several industrial fields. However, one major drawback of these alloys for nuclear applications is

the activation of Cobalt under neutron flux in a reaction $^{59}Co + (n, \gamma) \rightarrow {}^{60}Co$. With a period of 5.7 years, the activity of Cobalt 60 is maximum during the operation of the reactor. A period of at least 30 years after the shutdown is necessary to observe a significant reduction of induced activity. Thus, it is desirable to avoid these alloys for severe neutron flow and different studies tried to find substitute material without cobalt or in very small quantities.

There are different areas in SFR that have been identified as being most affected by friction (wear) as the strongback support on the primary vessel, candles assembly components, steam generator components, moving parts in valves…

The requirements are very demanding: tribology and corosion under sodium, operating temperature from 180 to 500°C, risk of thermal shock and thermal cycling, and life time of over 60 years without binding or degradation. Considering the tribological tests needed to analyze the wear behavior of the couple of materials in contact, if a tribometer for tests under liquid sodium is setup and currently in evaluation, we have decided to make tribological test under argon gas protection.

As we have said and following the results of previous studies, it has been demonstrated that, if the oxygen content is carefully controlled (for example by oxygen trapping devices) and temperature ≤500°C, as it is planned for the future reactor, the liquid sodium will have a very minor corrosion effect on the materials under study (ref. C. Latge [1], [2]).

Moreover, as it will be presented in this article, the specifications of the contacts selected for the study show a heavy load which substantially prevents the formation of a liquid film lubricant. Additionally considering the low viscosity of the liquid sodium, the inert atmosphere appears to be a good substitute to liquid sodium for the wear tests.

II. SELECTION OF MATERIALS AND PROCESS

II.A. Stellite® Alloys

Stellite is the well known and widely used hardfacing wear resistance material. The Stellite alloy, from Deloro Company, is a cobalt-chromium base specially designed for abrasion resistance. There are many alloys of Stellite composed of variable proportions of cobalt, nickel, iron, aluminum, boron, carbon, chromium, manganese, molybdenum, phosphorus, sulfur, silicon and titanium, most alloys having four to six of these elements. The Stellite alloy is nonmagnetic and has very good corrosion resistance. The different alloys have been optimized for different applications.

Stellite alloys have a high melting point and high hardness (eg Stellite 6: 40 HRC, melting point 1260°C-1357°C). They are therefore very difficult to machine. The hardness is strongly dependent on microstructure. The ductility of Stellite is mainly determined by the volume fraction of carbides and their morphologies. An increase of carbides reduces ductility. Under conditions of oxidation, the elements Cr and Co can form chromium and cobalt oxides at different oxidation levels [1,3]. The abrasion resistance is proportional to the hardness and increases with the proportion and size of carbides [4,5].

A large number of Stellite substitutes has been proposed in the literature. Considering requirements, thick coatings are preferably retained. Among them, we can consider two main types of materials: the iron or nickel based alloys.

Stellite alloys are quite well known and widely used with Laser Cladding. For the study, the parameter selected are as indicated in table 1:

Material	Laser power (W)	Travel speed (m/min)	Powder flow (g/min)
Stellite6 Laser	600-800	1	3-6

Table 1: Selected process parameters for Laser Cladding of Stellite6

If iron base alloys cannot be definitely excluded, the bibliography [6,7,8] mainly demonstrates the poor behavior of the iron-based hardfacing coatings at high temperature regardless of the deposition process.

At the opposite, authors have evidenced the interest of using Nickel based alloys for replacing the Cobalt based ones [9,10]. Because of that, we have selected one promising nickel base alloys: Colmonoy®5.

II.B. Colmonoy®

The Colmonoy is a nickel-based alloy developed by Wallcolmonoy Company which comprises hardening chromium borides and carbides [11]. Its main interest is to be Cobalt free while providing different grades adapted to different wear and corrosion conditions.

For most of the Colmonoy alloys, the metallurgical analysis shows the presence of many borides and carbides, especially CrB, in a solid solution of γNi. Although partial, the tribological tests exhibited satisfactory results (conducted at room temperature).

The alloy can be deposited by different processes. However, the aim to obtain a dense deposit, to better control and, potentially, automatize the process leads to investigate the fusion processes. Two processes are investigated in the study: Plasma Transferred Arc welding (PTA), and the Laser Cladding.

PTA has been widely investigated and used in the industry. Experiences and drawbacks on application of PTA for hardfacing materials exist. Obtaining sound clads is reached by starting on existing process parameters from previous experiences and optimization steps. Therefore, the realization of the sample by PTA will not be presented in detail in the following sections.

Laser Cladding is selected for specific application that requires improvements in quality of deposited materials, quality of the geometry of the clads, limitation of distortion,…Indeed, Laser Cladding can provide interesting properties: the dilution of substrate can be accurately controlled and reduced, high solidification speed and thermal gradient can give a very fine microstructure with homogeneous properties and higher hardness. [13].

For example, Ming et al. [11] present a study of Colmonoy 6 and 88 (17.3% grade tungsten) coating on AISI 1020 by Laser Cladding. The results show very good density and cohesion of the coating. The authors also show that the behavior of the coating depends more on the nature and proportion of the main hardening phase rather than the average macro hardness of the material. Of course, this is strongly conditioned by the process parameters.

Considering the potential interest of the Laser cladding, it has been decided to make a process parameter search for the proposed material that is presented in the next section.

II.C. Laser Cladding process parameter search

The process consists of two essential parts: melt pool formation and fusion by a moving laser beam and supply of cladding material to the substrate. Its main problem with this process is the number of parameters and their influence on the quality of the clad tracks. It involves a lot of parameters. Among them, three main parameters are the speed processing, the powder feeding rate, the laser power.

II.C.1 Experimental setup

The test system is shown in the figure 1. In this project, the continuous YAG laser was used to make deposits. Nd:YAG laser have been developed to laser powers of several kWs, making them useful for laser surface treatments.

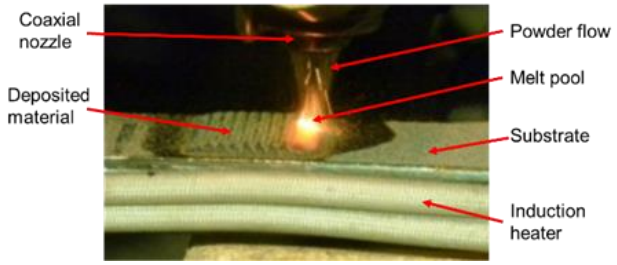

Figure 1: Laser Cladding setup

The wavelength of 1.064 µm is more efficient: absorption on a solid steel surface is about 30%. Under cladding conditions the absorption increases to 60%. Another advantage of solid-state near infra-red lasers is the possibility to transport the laser beam through optical fibers, allowing flexible beam handling systems. The laser beam is at the center of the cladding nozzle. The metal powder is added by the black tube. They are transported by a gas stream and injected into the melt pool. On the way through the laser beam, they absorb laser energy. The inert gas was used to avoid contact of the liquid bath with the area. This contact causes the oxidation. The substrate was preheated by a heating plate.

II.C.2 Selection of process parameters

For the experiments, specimens of 316L steel (50x50x10 mm and 200x50x20 mm) were used as substrates. The particle size of Stellite 6, and Colmonoy 5 are between 45µm and 75µm. The thickness of the cladded materials is expected to be >4mm.

For the first campaign of the parametric search for Colmonoy 5, the initial parameters were selected to produce thin deposits. Their thickness is between 0.3-1.5mm. Initially, a high travel speed, a low laser power and a low powder feeding rate have been used. Unfortunately, the clads were cracked and contained a high number of porosities, including big porosities (diameter > 50µm).

In order to avoid or to reduce these phenomena, we had to analyze the causes of each one.

II.C.3 Porosity

There are many factors that increase the porosity of the clads:

- Water adsorbed on the powder. The way to avoid it is mainly to preheat the powder before and during the cladding. This has been applied in our experiment by heating the powder at about 80-100°C all along the process.
- Included gas in the powder. Sometimes, atomization gas can be trapped into the powder during formation of the grains. If the powder is used, the occluded gas can be present in the melt pool. Depending of the

movement of the liquid metal in the pool, the occluded gas can be moved to the surface or inside the melt pool. In the second case, this occluded gas can generate porosities during solidification. The way to avoid this is to enlarge the melt pool. This allows the occluded gas to move to the surface of the melt pool.

- Fusion conditions can lead to the formation of porosities. This is the case, for example, if there is a lack of energy for the fusion of the powder. Therefore, it is important to keep a sufficient energy linked to the powder flow rate.

The analysis of the porosity in the powder was carried out. It is a factor that increases the porosity in the clad.

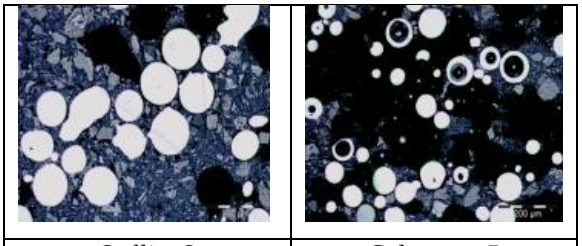

Stellite 6	Colmonoy 5

Figure 2: Micrography of the 2 powders selected in the study

Colmonoy 5 has a higher number of porosities compared to Stellite6 powder, including big ones (see figure 2). This depends on the method of powder production.

Furthermore, as it has been said, the small size of the melt pool also tends to increase the number of porosities of the clad.

Consequently, it has been decided to change the process parameters in order to increase the size (particularly the length) of the malt pool

II.C.4 Crack and deformation

In the initial trials, the produced clads exhibit cracks, as for example in figure 6. After analysis, it is clear that these cracks are coming from hot cracking causes but certainly from stress produced the deposition.

In order to avoid this, it has been considered to preheat the substrate between 400°C-600°C and cooling the substrate with low cooling rate after the cladding process;

Another way to artificially decrease the stress has been to introduce an initial opposite stress by making fusion lines at the back side of the substrate for cladding.

In addition, crack susceptibility and distortion have been dramatically reduced by induction heating of the substrate at 400 to 550°C (before, during, and after cladding, before a low cooling sequence).

The samples produced in the fourth campaign of experiments are sound. In the fifth campaign, samples for tribology tests have been produced.

Moreover, we considered a techno-economical criterion trying to increase the deposition rate.

Another consideration was to control and limit the dilution of the substrate. This is important because the increase of iron content in the material could potentially badly influence the wear resistance of the alloy, especially at high temperature.

An example of the cross-section of a typical sample is shown in Figure 2. In most of the sample and processing conditions, the microstructure is globally homogeneous along the clad, from the substrate to the top. We can notice a coarser microstructure, exhibiting oriented columnar dendritic structure. This is not surprising and usually encountered in laser clads.

In all of the samples, the interface shows a good metallurgical bounding and continuity without defect. In figure 8, most of the clad (the interface excluded) consists in mostly equiaxed and thin structure.

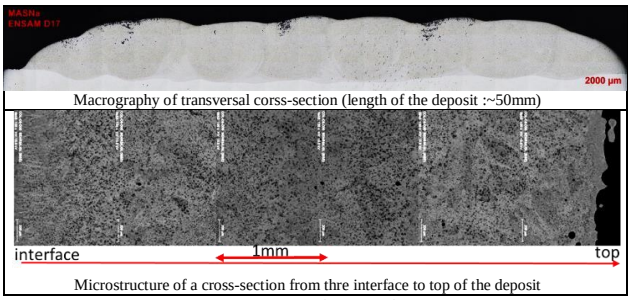

Figure 3: Micrography of a clad from the initial trials

Following different campaign of experiments, each problems has been tackled by tuning the process parameters. After optimization, the main process parameters selected are the following (table 2):

Material	Laser power (W)	Travel speed (m/min)	Powder flow (g/min)
Colmonoy5 Laser	1500-3000	1	18-24

Table 2 : Microstructure at near interface

More globally, it is clear that, even if PTA and Laser Cladding process parameters providing sound clads have been obtained, Colmonoy 5 exhibits a significant crack tendency that has to be taken into account in its potential selection as Stellite substitute.

II.C.5 Hardness and dilution

The hardness profile along the depth of cross-section in the coating was measured using a Vickers hardness tester with a load of 0.2kg and a loading time of 11.6s (Figure 4).

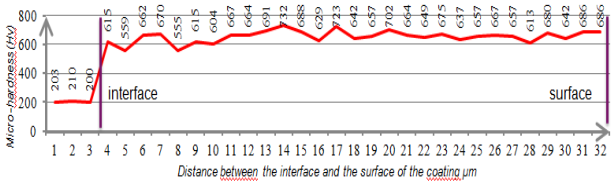

Figure 4: Microhardness profile of a typical clad from the interface to the top

Considering the parameter window, most of the samples exhibit a homogenous microhardness between 500 to 800 HV. Of course, the dilution of the iron from the substrate can lead to a decrease in microhardness.

Depending of the process parameters, profiles of iron content can be classified in three categories (Figure 5):

- At low travel speed (80-150mm/mn) and low powder flow rate (2-5g/min), the dilution is important and the transition between the substrate and the clad is quite smooth. The iron content goes from about 10% to the 316L iron content in about 1mm.
- When increasing travel speed to 200mm/mn, the dilution is decreased. The iron content in the clad slightly decreases but stay relatively high (about 10% instead of 3.8% in the powder). Moreover the dilution zone is reduced to less than 500µm.
- When increasing the travel speed (>200mm/min) and the powder flow rate (>5g/min), the dilution is very limited. The iron content in the clad becomes around 5% all long the clad and the dilution zone is limited to about 250µm.

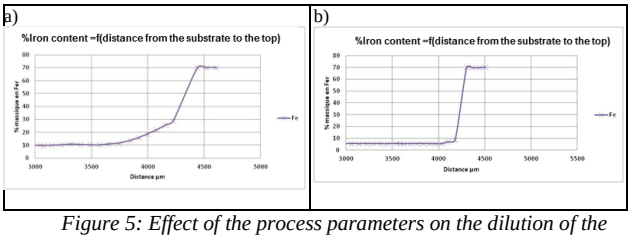

Figure 5: Effect of the process parameters on the dilution of the substrate by measuring the iron content (%weight) along the clad, a) high dilution, b) very low dilution

II.D. Microstructural analysis

Materials and methods

The following materials have been used for the material characterization:

- FEG-SEM for cross-section analysis
- WDS (Wavelengh Dispersive Spectroscopy) Accelerating tension 15kV. EDS could be also used to research boron but we have to work at low accelerating tension, typically 5 kV and without any possibility of quantification.

Microstructural analysis

No matter what deposition process was used, microstructures of Colmonoy alloys globally consist in three interlocked parts, a dendritic one, various precipitates in terms of size, shape and naturally chemical composition and finally several binary or ternary eutectics (see Figures 6, 7 and 8).

The main difference between PTA or Laser Cladding processes is the typical size and morphology of the microstructure and, not the nature of the created phases. Indeed, Laser Cladding microstructures are refined compared to the PTA ones which are coarser than Laser Cladding (see Figure 8 PTA)

The present microstructural analysis is focused on PTA coatings since the coarse-textured microstructure is easier to study and to understand the evolution during the cooling stage.

Based on the SEM observations, EPMA analysis but also on Ni-Cr-C, Ni-Cr-B and Ni-Si-B ternary equilibrium diagrams, the following solidification path with associated microstructure (Figure 6) is proposed:

$L \rightarrow M_7C_3 + CrB$ (or Cr_5B_3) + L1

$\rightarrow M_7C_3 + CrB$ (or Cr_5B_3) + γNi + L2

$\rightarrow M_7C_3 + CrB$ (or Cr_5B_3) + γNi + $(\gamma Ni + CrB)_E$ + $(\gamma Ni + Ni_3B)_E$ + L3

$\rightarrow M_7C_3 + CrB$ (or Cr_5B_3) + γNi + $(\gamma Ni + CrB)_E$ + $(\gamma Ni + Ni_3B)_E$ + $(\gamma Ni + Ni_3B + Ni_3Si)_E$

$\rightarrow M_7C_3 + CrB$ (or Cr_5B_3) + $(\gamma Ni + Ni_3Si_{(p)})$ + $(\gamma Ni + CrB)_E$ + $(\gamma Ni + Ni_3B)_E$ + $(\gamma Ni + Ni_3B + Ni_3Si)_E$

E stands for eutectic, P stands for precipitation in solid state and L stands for liquidus.

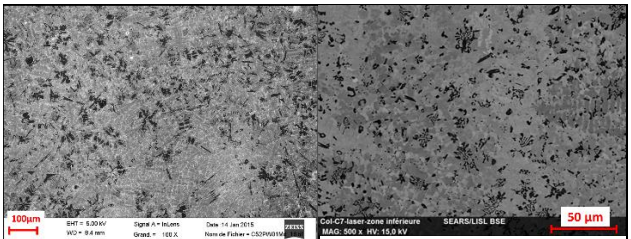

Figure 6: Colmonoy 5 microstructure, general view for PTA and Laser Cladding.

The different phases have been identified by local EPMA analysis. The measured chemical composition was then

compared to theoretical chemical composition. Despite some variations in global balance due to carbon contamination and the « matrix effect », the identified phases were in good agreement with the theory given by equilibrium ternary diagrams.

WDS chemical distribution maps were also performed to check the homogeneity of PTA microstructure (see Figure 10). At this scale of analysis, microstructure is quite homogeneous even if we can notice large sized chromium carbides and borides. These precipitates are primary precipitates which have developed at high temperature in the molten pool before the dendritic growth. On the same family of Colmonoy 5 coatings, if the temperature is not well controlled during deposition, primary precipitates could grown up to several hundreds microns. The solidification sequence went on with binary eutectic formations and finished with the ternary eutectic formation.

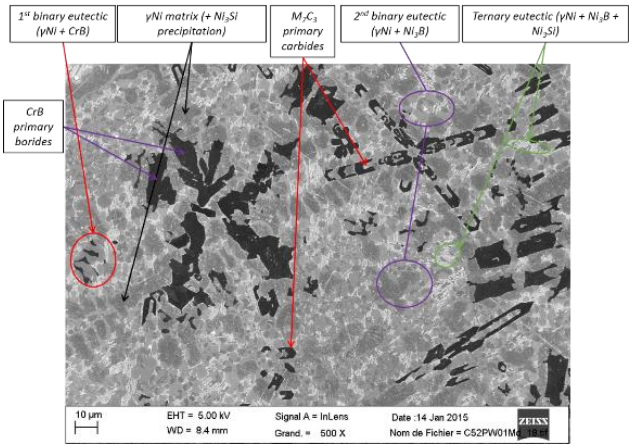

Figure 7: SEM view of Colmonoy 5 PTA microstructure (In Lens mode).

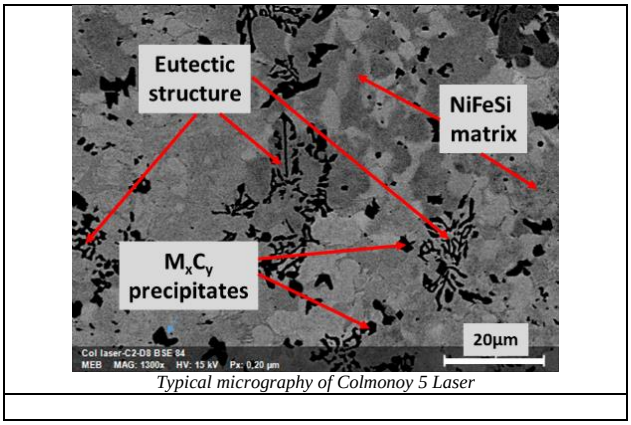

Typical micrography of Colmonoy 5 Laser

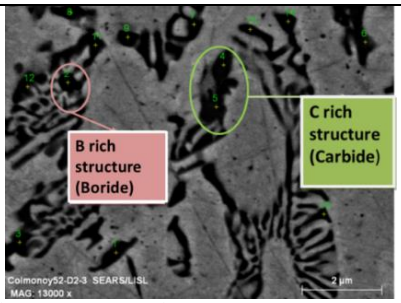

Detail of the microstructure of Colmonoy 5 Laser showing carbide and boride structures

Figure 8: SEM view of Colmonoy 5 Laser microstructure

Local investigations on dendritic matrix and eutectics (see Figure 9 and 10) were carried to point out the previous observations. The solubility of boron in nickel is almost inexistant. Thus, boron is used to form primary chromium borides if temperature of the molten pool is high enough, if not, boron is mainly used to form Ni_3B part of binary and ternary eutectics. (CrB+γNi) eutectic is also found but it remains in a lower proportion. The solubility of silicon in nickel can reach 9% wt. around 1100°C that is why, at a lower temperature, it is possible to have Ni_3Si precipitation in the γNi matrix.

From a pollution aspect, phophorus is mostly concentrated/segregated in the ternary eutectic which is the last liquid to solidify.

This metallurgical characterization is an essential aspect to understand to mechanical/tribological behavior of coatings. Indeed, the compromise between high hardness and induced mechanical fragility is not only controlled by large primary precipitates but more especially by Ni_3B boride which constitute a non-negligible part within the whole phases.

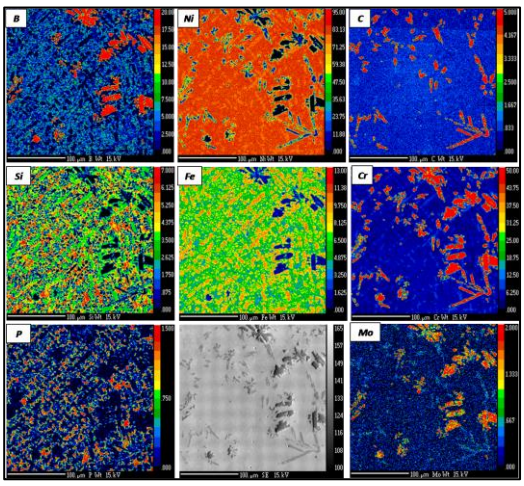

Figure 9: WDS chemical distribution maps for Ni, Cr, B, Si, C, Fe, Mo and P.

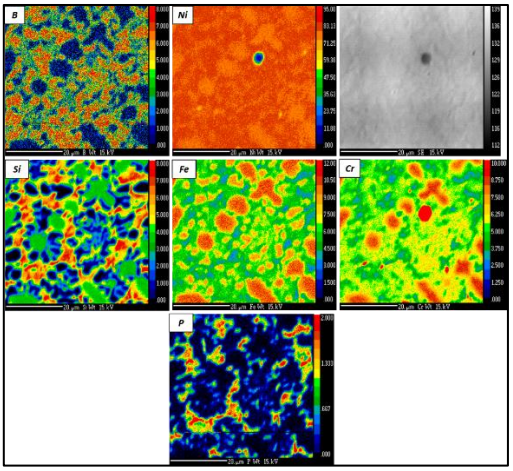

Figure 10 : WDS chemical distribution maps for Ni, Cr, B, Si, Fe, and P, details on matrix and eutectics.

III.TRIBOLOGICAL ANALYSIS

The project is ongoing and it has been decided at the beginning to design and implement a dedicated device for wear test under sodium at CEA.

However, in order to rapidly start and to simplify in the first step the wear tests, wear tests under Argon gas protection in temperature has started. Later on, the wear test under argon will continue in parallel to the sodium environment ones. This allow multiplying the wear configurations (materials, load, speed, temperature). As can be seen in the following sections, the wear configurations are as close as possible between the two systems.

III.A. Tribology under sodium

The tribometer under sodium is based on a symmetric loading system. The samples are placed in a moving axis up and down. Two arms supporting the pins are placed on the two sided and the load is applied symmetrically by masses. This system is placed in an oven container filled of liquid sodium. Figure 11 presents a general view of the tribometer. The parameters range are:

- Temperature : <650°C
- Travel speed : 10µm/s to 5mm/s
- Maximum sliding length : 15mm
- Maximum load : <45MPa
- Minimal load : 5 MPa
- Pin diameter (planar) : 5mm (316LN)

Currently, the tribometer under sodium is under testing. A particular attention is made to keep the oxygen content of the liquid sodium at the very low required level.

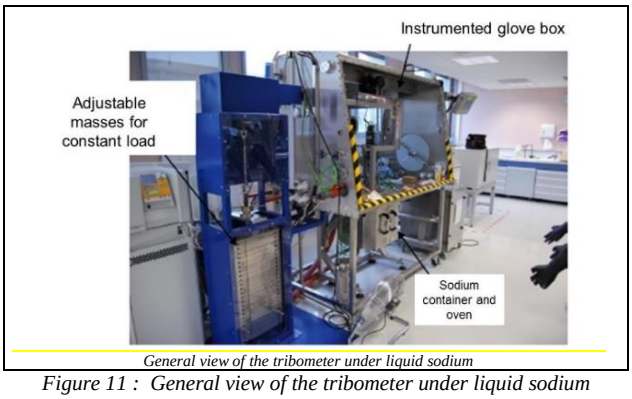

Figure 11 : General view of the tribometer under liquid sodium

III.B. Tribology under Argon

III.B.1 Experimental procedure

The tribometer under Argon gas protection (Figure 12) has been designed for equivalent characteristics to the Sodium tribometer.

On this device, the tests have been carried out with the following parameters (defined to be as close as posssible to the planned operating conditions):

- Temperature : 200°C
- Travel speed : 1mm/s
- Sliding length : 10m
- Maximum load : 31MPa
- Pin diameter (planar) : 5mm (316L(N))
- Argon gas protection

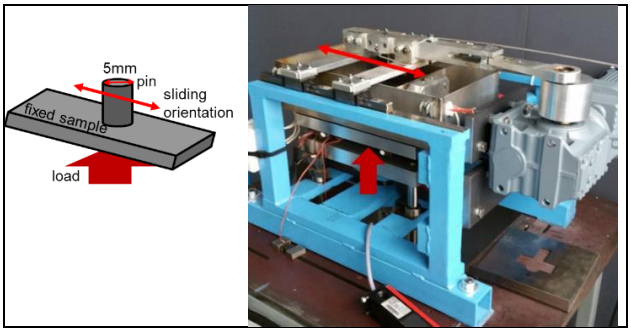

Figure 12 : Linear tribometer under Argon gas protection

The three deposits Stellite6, Colmponoy5 laser and Colmonoy 5 PTA have been tested.

The wear loss of the deposits was measured by a microtopography. Wear track of the samples and debris were examined by SEM/EDS to identify the wear mechanisms.

III.B.2 Wear mechanisms

As a first indication of the wear behaviour of the materials is shown by the evolution of the friction coefficient and by the loss of material on sample and pin after the 10m sliding.

The Figure 13 exhibits a difference for the evolution of the friction coefficient for the 3 materials. After an initial period, Stellite 6 shows the lower coefficient (~0.35-0.4) that remains constant.

Concerning Colmonoy 5, the PTA deposit shows a very constant and regular coefficient during sliding at a higher level (~0.55). The Colmonoy 5 Laser shows an evolving coefficient with some irregularities starting from a high level (~0.7) and decreasing step by step up to reach the Stellite 6 coefficient (~0.4).

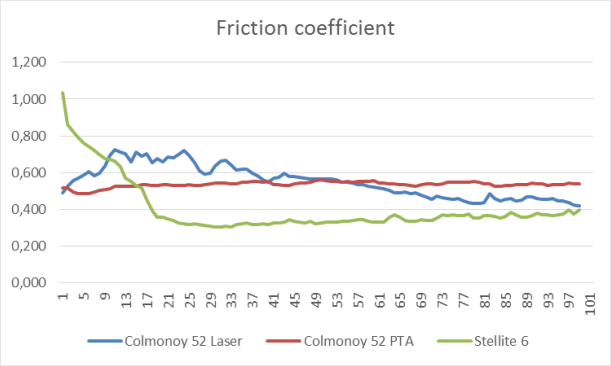

Figure 13 : Friction coefficient during sliding for the three materials (total sliding distance: 10m)

This is the sign of a transformation of the surface. This can be seen and confirmed by analysis of the wear loss (in Figure 14).

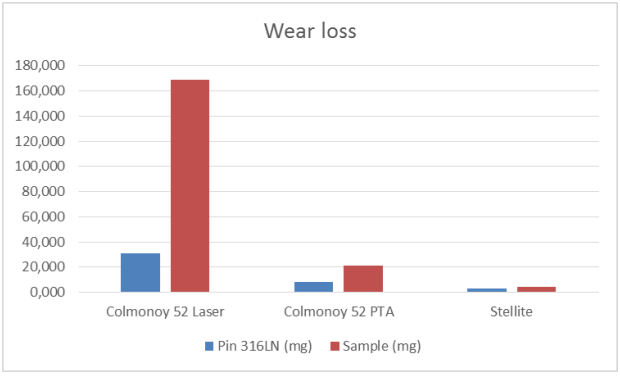

Figure 14 : Wear loss or the three materials and pins

First, it is clear that the Stellite 6 surface has the lower wear loss and the lower wear loss on pin too. This is shown in Figure 15. The surface remains relatively smooth after sliding. Some material (third body) has been clearly spread onto the surface, certainly by a combined adhesive and abrasive mechanism.

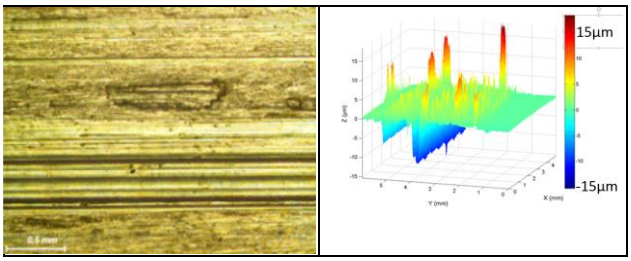

Figure 15 : SE micrograph characteristics of worn surface (left), and surface topography, of wear track for Stellite 6

Concerning the Colmonoy 5, a global dominant adhesive mechanism with a first abrasive period can be seen on the samples (laser and PTA). However, the wear loss is much higher on Colmonoy 5 laser (Figure 16) than in Colmonoy 5 PTA (Figure 17), and both for the 316LN pin.

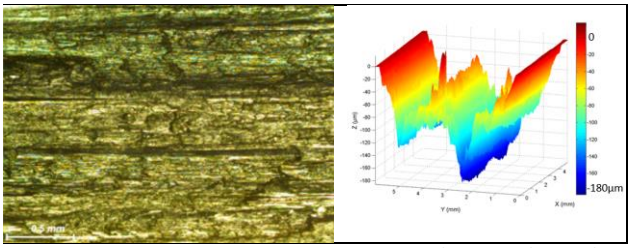

Figure 16 : SE micrograph characteristics of worn surface (left), and surface topography, of wear track for Colmonoy 5 laser

For both samples, the surface is considerably machined with a significant presence of groves. A closer analysis of the surface shows that, probably, its degradation occurs from micro-cracks on borides and carbides (to be confirmed), that generates hard debris that play the abrasive role.

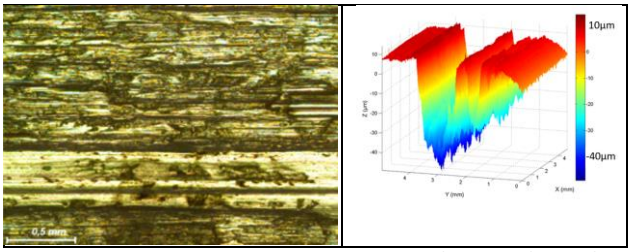

Figure 17 : SE micrograph characteristics of worn surface (left), and surface topography, of wear track for Colmonoy 5 PTA

A closer analysis of the surfaces by WDS indicates a presence of deposited iron on Colmonoy 5 laser and not on Colmonoy 5 PTA.

The difference of the wear behavior between Colmonoy 5 laser and Colmonoy 5 PTA is certainly related to the difference of microstructure in size and nature. As it has been shown, the Colmonoy 5 laser has a refined microstructure with small hard precipitates and a very small presence of eutectics surrounding them, in comparison to the Colmonoy 5 PTA. Thus, it can be

suggested that the high wear loss of Colmonoy 5 surface can be induced by to phenomena:

1. For Colmonoy 5 PTA, the surface is worn by an initial abrasive condition. Then, a third body mixing worn surface and iron coming from the pin is spread onto the surface by adhesion.
2. For Colmonoy 5 laser, the surface is worn by an initial abrasive condition. Then a third body mixing the two worn material (Colmonoy 5 and 316L(N) from pin) and containing a higher proportion of iron is deposited. During a second phase, this third body is partly detached form the surface during sliding and the process restarts, generating a higher degradation of the material.

IV. CONCLUSION

In this article, we have presented a new study on Cobalt-free hardfacing materials for Fast Sodium Reactors. Some nickel based alloys have been selected. PTA and Laser Cladding processed is used for cladding the alloy onto the substrate (316L or 316L(N)).

The parameter search for Laser Cladding has been presented for Colmonoy 5 alloy. We have demonstrated that this alloy can be deposited and that sound clads (no crack, few porosities) can be obtained.

The metallurgical analysis has been initiated and first results exhibit a thin microstructure globally equiaxed, with a good homogeneity from the interface to the substrate up to the top of the clad. hardening phases (carbides and borides) are uniformly dispersed into the material.

A solidification process has been proposed for explaining the Colmonoy 5 microstructure for PTA. It is clear that the main difference in the materials obtained by the two processes is in the refined microstructure induced by the higher solidification speed and higher cooling rate for Laser Cladding than for PTA.

Nevertheless, The work in ongoing to analyze the microstructure of the two deposits at higher magnification to check for potential differences.

Tribology tests under gas protection have been undertaken in the three evaluated materials. Wear mechanisms have been proposed for each material. However, a deeper investigation is in progress in order to verify the proposed hypothesis on wear mechanisms (cross-section analysis, EBSD …).

Of course, scale one wear test under sodium is required for making a final comparison and validation of the materials. Consequently, the design of a scale one tribometer under Sodium is started. Meanwhile, investigation the laboratory scale tribometer under sodium will continue to enforce our knowledge of the wear behaviour of the selected materials.

ACKNOWLEDGMENTS

The authors thank very much Jérome Varlet from CEA/DPC/SEARS/LISL and Christian Cossange from EDF/R&D/MMC for their help for material analysis, and Ibrahim Demirci, from Arts et Métiers ParisTech, MSMP Laboratory, for the tribological tests and analysis.

REFERENCES

1 P.M. Dunckley, T.F.J. Quinn, and J. Salter, Studies of the Unlubricated Wear of a Commercial Cobalt-base Alloy at Temperatures up to about 400°C, ASLE Transactions, 19(3), (1976), pp. 221-231

2 F. Rouillard, B.Duprey, R. Robin, L. Nicolas, P. Aubry, C. Blanc, M. Tabarand, H. Maskrot, M. blat-Yriex, G. Rollonad, T. Marlaud, Evaluation of Cobalt Free Coatings as Hardfacing Material Candidates in Sodium Fast Reactor and Effect of Oxygen in Sodium on the Tribological Behaviour, IAEA-CN-245-126, FR17, Yekaterinburg, Russian Federation , June (2017)

3 H. So, C.T. Chen, and Y.A. Chen, Wear Behaviours of Laser-clad Stellite Alloy 6, Wear, 192(1-2), (1996), p. 78-84

4 J.T.M de Hosson, and L. de Mol van Otterloo, Surface Engineering with Lasers of Co-base Materials, Surface Treatment, Computer Methods and Experimental Measurements. Comput. Mech. Publications, Southampton, UK, (1997), pp. 341-59

5 de Mol van Otterloo, J.L. and J.T.M. de Hosson, Microstructure and abrasive wear of cobalt-based laser coatings, Scripta Materialia, 36(2), (1997), pp. 239-45

6 D.H.E. Persson, S. Jacobson, S. Hogmark, Effect of temperature on friction and galling of laser processed Norem 02 and Stellite 21, Wear 255, (2003), pp.498–503

7 D. H. E. Persson, Laser processed low friction surfaces, Dissertation for the degree of Licentiate of Philosophy in Materials, Materials Science Division, the Ångström Laboratory, Uppsala University, Sweden, March (2003)

8 C. B. Bahn, B. C. Han, J. S. Bum, I. S. Hwang, Chan Bock Lee, Wear performance and activity reduction effect of Co free valves, in PWR environment, Nuclear Engineering and Design 231, (2004), pp. 51–65

9 M. Corchia, P. Delogu, & F. Nenci,. Microstructural Aspects Of Wear-Resistant Stellite And Colmonoy Coatings by Laser Processing, Wear, Volume 119, pp. 137-152, 1987

10 Kashani, A. Amadeh, & H. Ghasemi, Room and high temperature wear behaviors of nickel and cobalt base weld overlay coatings on hot forging dies. Wear, 262(7-8), pp. 800-806, 2007

11 Qian Ming, L.C. Lim, Z.D. Chen, Laser cladding of nickel-based hardfacing alloys, Surface and Coatings Technology 106, (1998), pp. 174–182

12 D. Kesavan, & M. Kamaraj, The Microstructure and High Temperature Wear Performance of a Nickel Base Hardfaced Coating, Surface and Coatings Technology, 204(24), pp. 4034-4043, 2010

13 C. Navas, R. Colaço, J. Damborenea, & R. Vilar, Abrasive Wear Behaviour of Laser Clad and Flame Sprayed-Melted NiCrBSi Coatings, Surface and Coatings Technology, 200(24), pp. 6854-6862, 2006

14 K. Komvopoulos, K. Nagarathnam, Processing and Characterization of Laser-Cladded Coating Materals, J. of Engineering Materials and Technology, vol. 112, pp. 131-143, 1990